

Study of the Diffusion Behavior of Seawater Absorption in Multi-Walled Carbon Nanotubes/Halloysite Nanotubes Hybrid Nanofillers Modified Epoxy-Based Glass/Carbon Fiber Composites

Praful Choudhari*, Vivek Kulkarni, Sanjeevakumar Khandal

Department of Mechanical Engineering, Sanjay Ghodawat University, Atigre, Kolhapur, Maharashtra, India

Email: *praful.choudhari@sanjayghodawatuniversity.ac.in, kulkarni.vv@sginstitute.in, khandal.sv@sanjayghodawatuniversity.ac.in

How to cite this paper: Choudhari, P., Kulkarni, V. and Khandal, S. (2024) Study of the Diffusion Behavior of Seawater Absorption in Multi-Walled Carbon Nanotubes/Halloysite Nanotubes Hybrid Nanofillers Modified Epoxy-Based Glass/Carbon Fiber Composites. *Modern Mechanical Engineering*, 14, 25-38.

<https://doi.org/10.4236/mme.2024.142003>

Received: January 30, 2024

Accepted: March 25, 2024

Published: March 28, 2024

Copyright © 2024 by author(s) and Scientific Research Publishing Inc. This work is licensed under the Creative Commons Attribution International License (CC BY 4.0).

<http://creativecommons.org/licenses/by/4.0/>



Open Access

Abstract

In the maritime industry, cost-effective and lightweight Fiber Reinforced Polymer (FRP) composites offer excellent mechanical properties, design flexibility, and corrosion resistance. However, their reliability in harsh seawater conditions is a concern. Researchers address this by exploring three approaches: coating fiber surfaces, hybridizing fibers and matrices with or without nanofillers, and interply rearrangement. This study focuses on evaluating the synergistic effects of interply rearrangement of glass/carbon fibers and hybrid nanofillers, specifically Multi-walled carbon nanotubes (MWCNT) and Halloysite nanotubes (HNT). The aim is to enhance impact properties by minimizing moisture absorption. Hybrid nanocomposites with equal-weight proportions of two nanofillers: 0 wt.%, 1 wt.%, and 2 wt.% were exposed to seawater for 90 days. Experimental data was subjected to modelling through the application of Predictive Fick's Law. The study found that the hybrid composite containing 2 wt.% hybrid nanofillers exhibited a 22.10% increase in impact performance compared to non-modified counterparts. After 90 days of seawater aging, the material exhibited enhanced resistance to moisture absorption (15.74%) and minimal reduction in impact strength (8.52%) compared to its dry strength, with lower diffusion coefficients.

Keywords

Glass/Carbon Fiber Hybrid Composites, Multiwall Carbon Nanotubes (MWCNTs), Halloysite Nanotubes (HNTs), Diffusion Behaviour, Impact Properties, Seawater Aging

1. Introduction

Fiber Reinforced Polymer (FRP) composites have become the preferred choice in the maritime sector, driven by technological advancements. Utilizing predominantly glass and carbon fibers, FRP dominates marine applications for decks, bulkheads, propellers, and machinery due to superior mechanical properties, flexibility, and chemical resilience [1] [2] [3]. Its prevalence in shipbuilding over steel and aluminium is attributed to cost-effective glass fibers and hybrid composites with carbon fibers. However, susceptibility to seawater-induced deterioration in mechanical performance necessitates ongoing research for improvement through various approaches like coating [4], hybridization [5] [6], and interply rearrangement [7].

Coating the surfaces of fibers is crucial to enhance interfacial performance in marine structures. Ester, polyurethane, gel coat, and epoxy coatings contribute to improved composite durability. The application of nano fillers such as silica, graphene oxide, alumina, nanoclay, and carbon nanotubes through spray coating enhances flexural, fracture, and impact resistance, especially in the face of seawater aging.

Hybridizing reinforcements in composites offers cost efficiency and customization. The combination of glass and carbon fibers enhances strength and reduces weight compared to plain glass fiber composites. Recent research has focused on improving epoxy properties by integrating nanofillers, with carbon nanotubes (CNTs) and halloysite nanotubes (HNTs) demonstrating promise. CNTs address brittleness and cracks in epoxy resin, providing enhanced mechanical properties in fiber polymer composites, including strong adhesion, customizable features, high modulus, elevated temperature resistance, and low creep [8] [9] [10]. Even at low levels, CNTs significantly improve toughness mechanisms in composite interfaces [11]. Bal *et al.* [12] studied the inclusion of a small amount of MWCNT in epoxy-based composites, revealing maximum degradation at 60 - 120 days, with 0.5 wt.% MWCNT showing the least deterioration. Nayak *et al.* [13] investigated the synergistic effects of Al_2O_3 and TiO_2 nanofillers in glass fiber epoxy composites exposed to seawater at 70°C for 40 days, reducing water diffusion coefficient by 12%. Residual flexural strength increased by 19%, and interlaminar shear strength by 21%.

Utilizing interply rearrangement as a crucial design optimization strategy significantly improves mechanical properties. In their study, Jesthi and Nayak [7] investigated the rearrangement of interplies such as $[\text{GCG}_2\text{C}]$, $[\text{G}_3\text{C}_2]_s$, and $[\text{G}_2\text{C}_2\text{G}]_s$, incorporating glass fiber on the top layer and carbon fiber in hybrid composites laminate over a 90-day period of seawater immersion at room temperature. The findings highlighted that the $[\text{GCG}_2\text{C}]$ hybrid composite demonstrated superior overall mechanical properties and minimal seawater absorption compared to other hybrid composites. This makes it particularly advantageous for applications in ship frames and marine structures.

While existing research has explored individual approaches like structural rearrangement and nanofiller effects on hybrid composite performance, the combined impact of these two approaches in the marine environment remains unexplored. This study addresses the gap by examining the synergistic effects of (MWCNT + HNT) hybrid nanofillers and structural rearrangement on glass/carbon reinforced epoxy composites. Composites were fabricated using compression molding techniques, including plain glass and carbon fibers, hybrid composites with interply rearrangement, and variations with nanofillers. The research focuses on understanding the impact properties, moisture absorption, and diffusion behavior under seawater-aged conditions over 30, 60, and 90 days.

2. Experimental Work

2.1. Materials

The current study utilized primary reinforcements as bi-directional woven fabric E-glass fibers (400 gsm) supplied by Valmiera Glass UK Ltd and bi-directional carbon fabric (3 k plain weave, 200 gsm) from Marktech Composites Pvt. Ltd, Bangalore, India. The hybrid composite, comprising ten layers, maintained a 72:28 weight ratio of glass to carbon fibers. Both plain glass/carbon fiber composites and hybrid composites were constructed. The overall weight ratio of reinforcement fibers to epoxy polymer was 55:45. LY-556 epoxy polymer and W152 LR hardener from CF Composites, Mumbai, India, were blended in a 100:30 ratio. Refer to **Table 1** for detailed properties of the materials.

Nanofillers

The nanofillers MWCNTs and HNTs were used as secondary reinforcements. The MWCNTs, synthesized through chemical vapor deposition by AD-NANO Technologies Pvt. Ltd, Shivamogga, India, were employed. These MWCNTs possess an outer diameter ranging from 10 to 30 nm, an inner diameter of 5 to 10 nm, a density of 2.1 g/cm³, and a length exceeding 10 μm, with 99% purity. Halloysite nanotubes (HNT) from Sigma Aldrich Company, Bengaluru, India, feature diameters of 30 to 70 nm, lengths of 1 - 3 μm, a tube-like structure, a density of 2.53 g/cm³, and a surface area of 64 m²/g, making them suitable for reinforcing epoxy matrix composites due to their high aspect ratio and minimal percolation characteristics.

Table 1. Physical and mechanical properties of carbon fiber, E-glass fiber, and epoxy resin.

Properties/Grade	Density (g/cm ³)	Tensile Strength (MPa)	Tensile Modulus (GPa)	Elongation at Break (%)
E-Glass Fiber	2.54	3100 - 3800	65.5 - 73.8	4.0
Carbon Fiber	1.76	4900	230	2.1
Epoxy	1.32	83 - 93	3.42	-

2.2. Methods

2.2.1. Preparation of MWCNT/HNT Modified Epoxy

Achieving a uniform dispersion of nanofillers in high-density epoxy poses challenges due to increased viscosity. To overcome this, nanofiller powders (MWCNTs and HNTs) were dried, combined in equal weights (1 wt.% with 0.5 wt.% MWCNT + 0.5 wt.% HNT, and 2 wt.% with 1 wt.% MWCNT + 1 wt.% HNT), and subjected to mechanical stirring, magnetic stirring, and sonication. The modified epoxy resin underwent preheating, additional sonication to break agglomerates, cooling, and gradual mixing with the hardener. Vacuum degassing was employed throughout the process to prevent bubble formation, ensuring a uniform distribution of nanofillers.

2.2.2. Preparation of Glass/Carbon Modified Epoxy-Based Laminates

Fabrication of glass/carbon fiber epoxy laminates occurred through compression molding. The mold was treated with a release agent, and epoxy was subsequently applied to one side of the fiber mat. This was followed by the layering of another mat and compression. Hybrid composites with interply rearrangement of $[G_3C_2]_s$ comprised six glass layers and four carbon layers, while plain composites consisted of ten layers of either glass or carbon fiber. **Figure 1** showcases five symmetrical composites: the plain glass fiber epoxy composite (G-E), carbon fiber epoxy composite (C-E) unmodified glass fiber/carbon fiber epoxy composite (GC-E) N_0 with 0 wt.% of (0 wt.% MWCNT + 0 wt.% HNT) nanofillers, modified glass fiber/carbon fiber epoxy composite (GC-E) N_1 with 1 wt.% of (0.5 wt.% MWCNT + 0.5 wt.% HNT) nanofillers, and modified glass fiber/carbon fiber epoxy composite (GC-E) N_2 with 2 wt.% of (1 wt.% MWCNT + 1 wt.% HNT) nanofillers. The resulting composite laminates, were cut to the necessary dimensions following ASTM standards with a water jet cutting machine

2.3. Characterization of Composite

To explore the synergistic effect of hybrid nanofillers, MWCNTs, and HNTs on the diffusion behaviour and impact properties of epoxy-based glass/carbon composite laminates under the effects of seawater, the study adhered to ASTM standards, and the findings are elaborated in the subsequent sections.

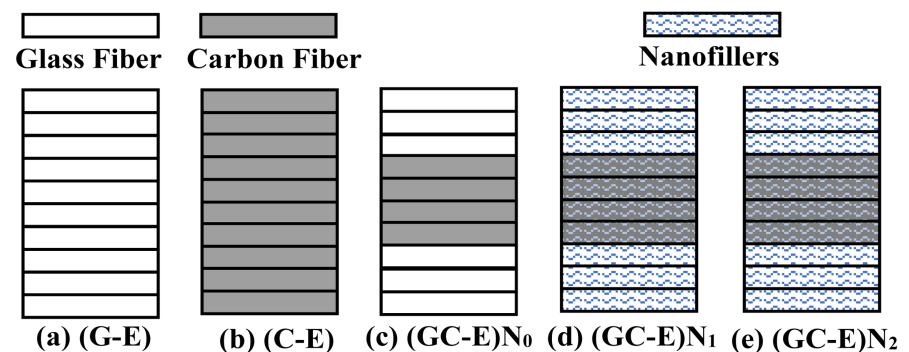


Figure 1. Interply rearrangement of composite laminates.

Moisture Absorption Study and Diffusion Behaviour

To simulate the marine environmental condition, natural seawater was collected from the Arabian Sea, Shrivardhan, India by placing inside a 40 liters fish tank as per the ASTM D5229 procedure. The pH of seawater was determined to be 8.37. The composites were immersed in seawater at room temperature for 90 days. Moisture absorption specimens were prepared following ASTM D 5229 procedures. The weights of all the composite type samples were measured using a precision balance ("LWL Germany") with least count 0.0001 g accuracy. At regular intervals, samples were removed, wiped with a cotton cloth to prevent water desorption, and promptly reweighed. Specimen edges were sealed with resin before seawater exposure to mimic real-world scenarios like ship hulls. This precaution aligns with practicality, ensuring the study focuses on one-dimensional absorption in composite materials subjected to wear or cracking. The percentage of moisture absorption after each period is expressed as the weight gain of the sample as a function of time, as mentioned in Equation (1)

$$M_t (\%) = \frac{W_t - W_0}{W_0} \times 100 \quad (1)$$

Where, M_t is the percentage of moisture absorption after each interval of time, W_0 is the weight of the dry sample (before seawater immersion) and, W_t is the weight of the wet sample at time t (after seawater immersion).

The water content (M_t) at any time (t) is determined through gravimetric analysis as per the given Equation (2). If diffusion occurs at a constant temperature and relative humidity, the water content (M_t) in a thin, flat plate specimen is described by the classical Fickian diffusion model [14] [15]. The experimental data were fitted using the traditional Fickian diffusion model [16]. This expression is applicable for both absorption and desorption, where M_t is:

$$M_t = G(M_\infty - M_i) + M_i \quad (2)$$

where:

M_t : Percentage moisture gain at time t .

M_∞ : Maximum moisture content achievable under the specified conditions.

M_i : Initial moisture content of the specimen.

G : Time-dependent parameter expressed as

$$G = 1 - \frac{8}{\pi^2} \sum_{n=0}^{\infty} \frac{\exp\left[(2n+1)^2 \pi^2 \left(\frac{-Dt}{h^2}\right)\right]}{(2n+1)^2} \quad (3)$$

where:

D : diffusion coefficient in the direction normal to the surface.

h : thickness of the specimen.

If diffusion occurs on both parallel faces, the specimen thickness is denoted by (h). Conversely, if one face is insulated with a water-impermeable coating, the specimen thickness is expressed as $2h$. Efforts have been made to simplify Equation (3) further, and an approximation has been proposed by Shen and Springer

[17], as illustrated in **Figure 2**. The simplified time-dependent parameter expressed in Equation (4).

$$G = 1 - \exp \left[-7.3 \left(\frac{-Dt}{h^2} \right)^{0.75} \right] \tag{4}$$

Moisture diffusion in FRP composites commonly exhibits anisotropic behavior, featuring faster diffusivity in the fiber direction as opposed to the transverse direction. The moisture diffusivity or diffusion coefficient (D) is determined through the moisture absorption curve using Equation (5) [4].

$$D = \left(\frac{h}{4 \cdot M_\infty} \right)^2 \left(\frac{M_2 - M_1}{\sqrt{T_2} - \sqrt{T_1}} \right)^2 \tag{5}$$

where:

h : specimen thickness,

M_∞ : weight of the saturated specimen and,

M_1 and M_2 : moisture absorptions at time T_1 and T_2 , respectively.

In the initial stage of moisture diffusion, the relationship between M_t and square root of time exhibits linearity, reflecting the independence of the diffusion coefficient on water content. The slope of this linear segment of the curve contains information about the diffusivity, as indicated by the Equation (6) below:

$$\text{slope} = \frac{M_2 - M_1}{\sqrt{T_2} - \sqrt{T_1}} \tag{6}$$

In the assessment process, the absorption of water along the width (w) and length (l) of the sample was disregarded. Nonetheless, under real-world conditions, seawater diffusion occurs in both the length and width directions. Consequently, the adjusted diffusion coefficient is computed according to Rao *et al.* [18], as outlined in Equation (7), wherein water absorption along both the width (w) and length (l) directions is considered.

$$D' = \frac{D}{\left[1 + \frac{h}{l} + \frac{h}{w} \right]^2} \tag{7}$$

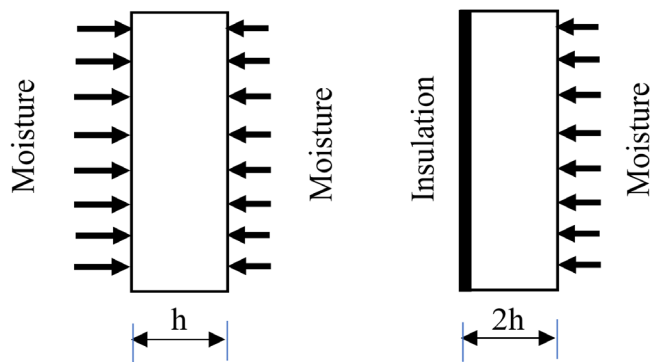


Figure 2. 2Moisture diffusion process [17].

3. Results and Discussion

3.1. Moisture Absorption and Diffusion Behaviour

The moisture absorption content is plotted against the square root of time ($t^{1/2}$) for different composite types following seawater exposure as shown in **Figure 3**. The findings indicate higher water absorption in the plain glass fiber (G-E) composite, with the plain carbon fiber (C-E) composite showing the subsequent highest absorption [19]. Both modified and unmodified hybrid composites exhibit lower water absorption compared to plain glass (G-E) or carbon fiber (C-E) composites.

Each curve displays an initial phase where moisture absorption content rises swiftly with the square root of time. Subsequently, a nonlinear phase follows, characterized by gradual increases in moisture content (%) until reaching a steady state. This initial behavior is distinctly governed by classical Fick's law, elucidating the moisture absorption mechanism in the early phase of moisture gain. An additional observation indicates that the moisture content in all composites was limited, as the coating on specimen edges prevented water infiltration into the laminate specimen. This observation aligns with the findings demonstrating that the presence of a coating layer reduces the moisture absorption content of composite laminates [20].

The findings indicate that the plain glass fiber (G-E) composite demonstrated increased moisture absorption content in impact (1.1564%) test specimens, with the plain carbon fiber (C-E) composite showing the subsequent highest absorption [19]. Conversely, the plain carbon fiber epoxy (C-E) exhibited reductions of 4.08% in impact test specimens, respectively, compared to the (G-E) composite. The unmodified hybrid glass/carbon fiber epoxy (GC-E)_{N₀} composites showed decreased moisture absorption content by 10.91% in impact test specimens, compared to the (G-E) composite.

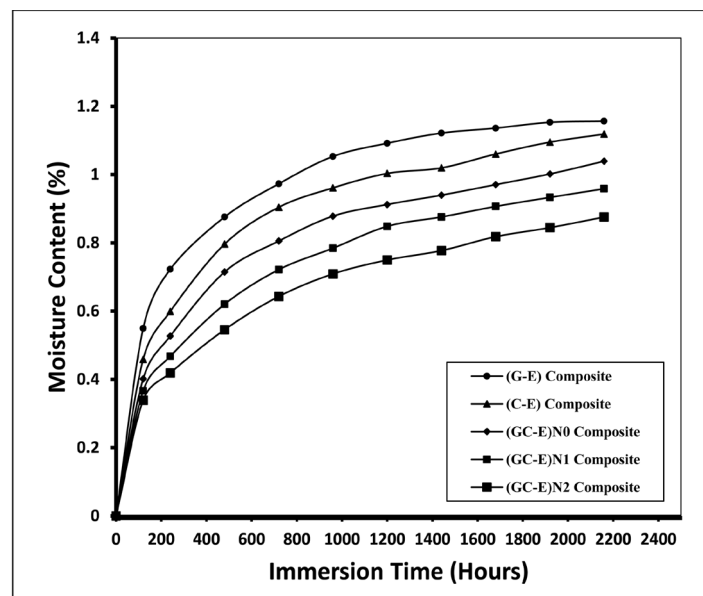


Figure 3. Seawater absorption versus time for different composite types.

In the case of hybrid composites, the water absorption is the highest for the unmodified hybrid (GC-E) N_0 type followed by the modified hybrid of (GC-E) N_1 and (GC-E) N_2 type.

Within the unmodified hybrid (GC-E) N_0 type, outer glass fiber layers enhance water absorption, while carbon fiber restricts it, reducing seawater absorption by reinforcing interface bonds and minimizing capillary action, aligning with Jesthi and Nayak's findings on interply rearrangement [7] [19]. The (GC-E) N_2 type exhibited the least moisture absorption, showcasing the synergistic impact of MWCNT and HNT nanofillers in hybrid composites offers valuable insights into their barrier properties to moisture, toughening mechanism, and improved bonding between hybrid fibers and modified epoxy.

The seawater diffusion coefficient was determined for all the types of fiber reinforced polymer composites using Equation (7) and is depicted in **Figure 4**. The highest diffusion coefficient was found to be 2.017×10^{-3} mm²/hour for (G-E) type composite. Nevertheless, the diffusion coefficient decreases for hybrid composites with and without nanofillers in comparison to plain GF and CF reinforced polymer composites. The lowest diffusion coefficient was found to be 1.287×10^{-3} mm²/hour for [GC-E] N_2 type hybrid composite in impact test specimen. In various studies, it's observed that incorporating nanofillers reduces the equilibrium water content in polymer systems, attributed to their superior barrier properties. The high aspect ratio of nanofillers creates a tortuous pathway, hindering water molecule diffusion [21]. The nanofiller's dispersion quality influences its occupancy in additional or free volume, with well-dispersed fillers enhancing the latter. Nanofillers in free volume effectively resist water absorption, explaining the superior water resistance of [GC-E] N_2 hybrid composites.

The moisture absorption content for all types of composite materials in the impact test specimens were calculated by mathematical model, as detailed in **Table 2**.

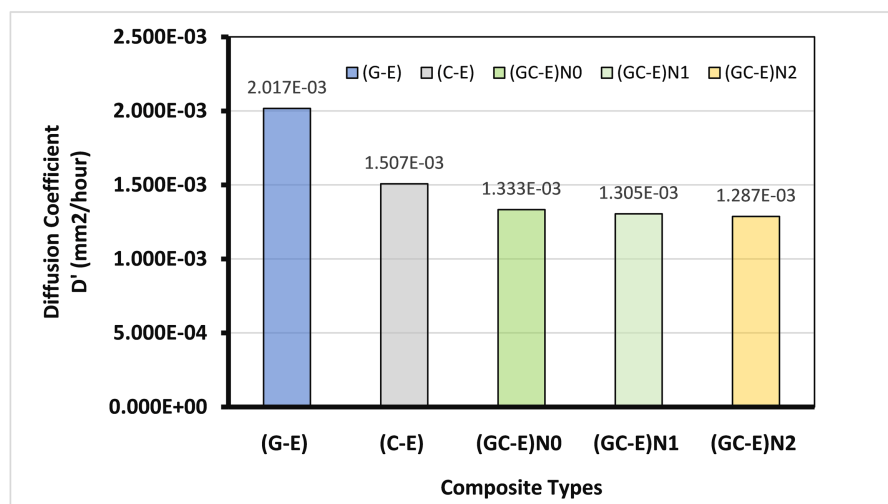


Figure 4. Diffusion coefficient versus composite type.

Table 2. Percentage moisture content for all the composite types of impact test specimens immersed in sea water.

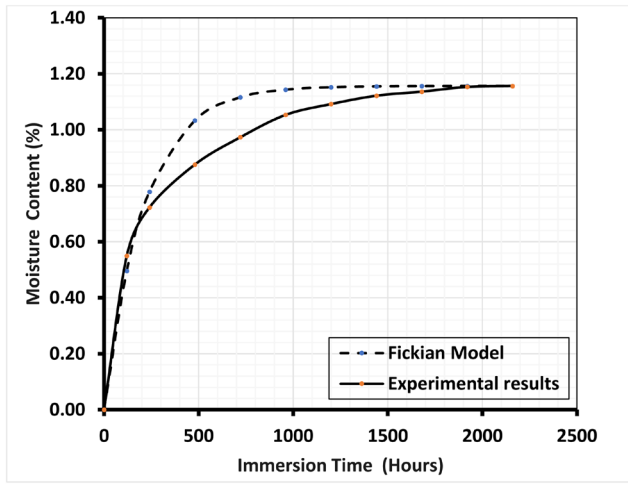
S.N.	Time of Immersion			Moisture Absorption Content (%) for composite Types				
	Sq. (hours)	hours	Days	(G-E)	(C-E)	(CG-E)N ₀	(GC-E)N ₁	(GC-E)N ₂
1	0.00	0	0	0	0	0	0	0
2	10.95	120	5	0.4953	0.3821	0.3211	0.2873	0.2714
3	15.49	240	10	0.7785	0.6337	0.5429	0.4901	0.4587
4	21.91	480	20	1.0329	0.9085	0.8022	0.7343	0.6771
5	26.83	720	30	1.1160	1.0276	0.9260	0.8559	0.7811
6	30.98	960	40	1.1432	1.0792	0.9852	0.9165	0.8306
7	34.64	1200	50	1.1521	1.1016	1.0134	0.9467	0.8542
8	37.95	1440	60	1.1550	1.1113	1.0269	0.9618	0.8654
9	40.99	1680	70	1.1559	1.1155	1.0333	0.9693	0.8707
10	43.82	1920	80	1.1562	1.1173	1.0364	0.9730	0.8733
11	46.48	2160	90	1.1564	1.1181	1.0379	0.9749	0.8745

The moisture content values obtained experimentally and those predicted by the mathematical model for impact test specimens as illustrated in **Figure 5**. **Figure 5(a)** showcases the results for pure glass fiber epoxy (G-E), **Figure 5(b)** for pure carbon fiber epoxy (C-E), **Figure 5(c)** for unmodified hybrid glass/carbon fiber epoxy (GC-E)N₀ composites, and **Figures 5(d)** and **Figures 5(e)** for nano-fillers modified (GC-E)N₁ and (GC-E)N₂ composites, respectively.

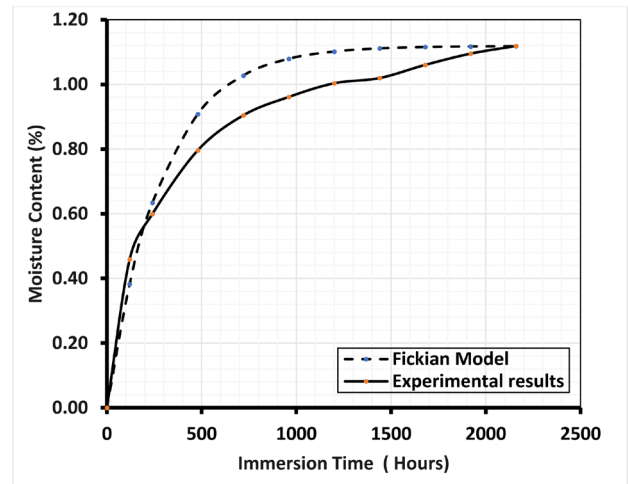
Figure 5 illustrates the use of the Fickian diffusion model in analysing the experimental data from impact tests in this study. The classic Fickian model, outlined in Equation (2), was expansively applied throughout the entire duration of test when employed on the experimental data. The theoretical approach utilized in this analysis is firmly based on the experimental data. The Fickian model is applied to fit the experimental data, with the solid lines in the figure depicting the experimental results. Meanwhile, the dotted lines represent the theoretical water absorption curves derived from Fick's law. Impact test specimens demonstrate a satisfactory correlation in both linear and saturation regions, with slight variations observed in the intermediate region. The percentage of absorption increases with the square root of the immersion time, a common phenomenon in the absorption process.

3.2. Effect of Moisture Absorption on Impact Properties

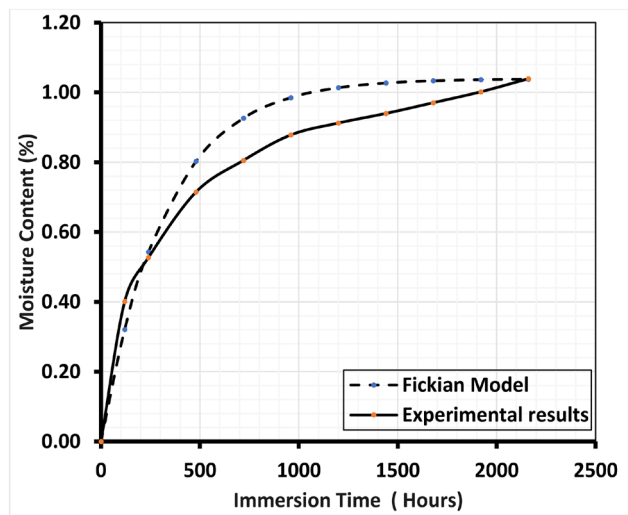
The specimen of all the five different composites was immersed in sea water for the period of 90 days at room temperature. The impact strength behaviour of the sea water aging specimen was recorded after 30 days, 60 days and 90 days of immersion. The impact test results in dry and seawater aged condition for various composite specimens are depicts in **Figure 6**, including pure glass fiber (G-E), pure carbon fiber (C-E), (GC-E)N₀, (GC-E)N₁ and (GC-E)N₂ composite impact energy absorption at the notch was measured.



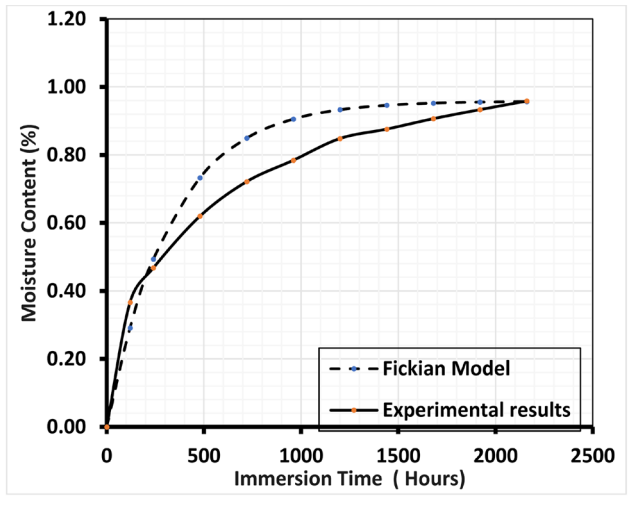
(a) (G-E) composite



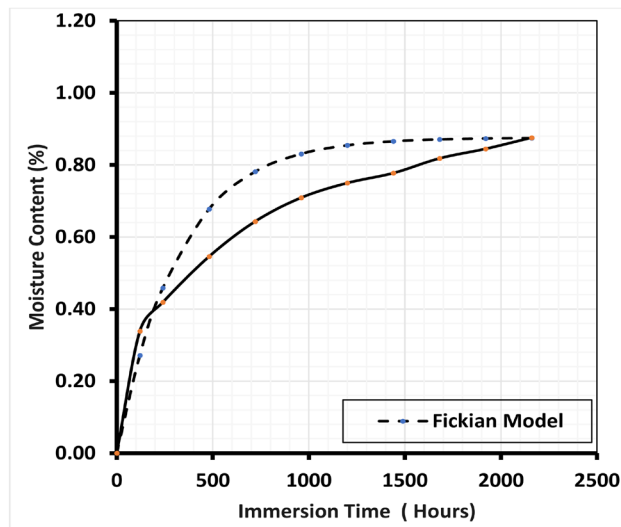
(b) (C-E) composite



(c) (GC-E) N_0 composite



(d) (GC-E) N_1 composite



(e) (GC-E) N_2 composite

Figure 5. Comparison of moisture content between experimental value and the predicted value by mathematical fick model.

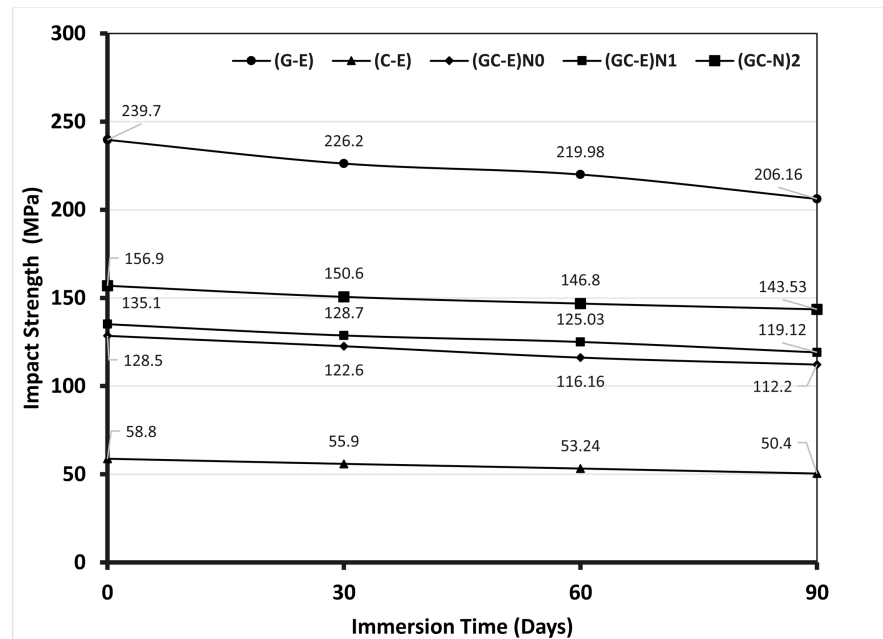


Figure 6. Comparison of impact strength of different composites under both dry and seawater-aged conditions.

In dry condition, the results revealed significant variations among the specimens. (C-E) composites exhibited the lowest impact strength at 58.8 KJ/m², while (G-E) composites displayed the highest at 239.7 KJ/m² due to the brittleness of carbon fibers. Following a 90-day immersion in seawater, the plain (G-E) composite exhibited the highest impact strength at 224.8 KJ/m², while the plain (C-E) composite recorded the lowest at 38.5 KJ/m². Over the 30-day, 60-day, and 90-day seawater aging periods, the impact strength of plain (G-E) decreased by 2.7%, 4.3%, and 6.2%, respectively. Conversely, the impact strength of plain (C-E) composite exhibited declines of 18.7%, 27%, and 34.6% over the same respective time frames. The hybrid composite (GC-E)N₀, featuring an interply rearrangement of glass and carbon fibers, demonstrated a significant 118.5% improvement in impact strength compared to plain (C-E) composites. However, when exposed to seawater, this enhancement decreased by 5%, 9.9%, and 15.3% over the periods of 30 days, 60 days, and 90 days, respectively.

The introduction of MWCNTs and HNTs enhanced impact strength, with (GC-E)N₁ composites experiencing a 5.1%, and (GC-E)N₂ composites experiencing a 22.1% improvement over unmodified (GC-E)N₀ hybrids, highlighting the synergistic effect of hybrid nanofillers and fiber interply in enhancing composite toughness. Nevertheless, when subjected to a 90-day period of seawater aging, the impact strength of (GC-E)N₀, (GC-E)N₁, and (GC-E)N₂ hybrid composites experienced decreases of 15.3%, 6.8%, and 4.5%, respectively, in comparison to specimens aged in dry conditions. Notably, the impact strength of (GC-E)N₂ hybrid composites showed a lower value compared to other hybrid composites in seawater aged conditions. This can be attributed to the lower moisture absorption content in (GC-E)N₂ hybrid composites.

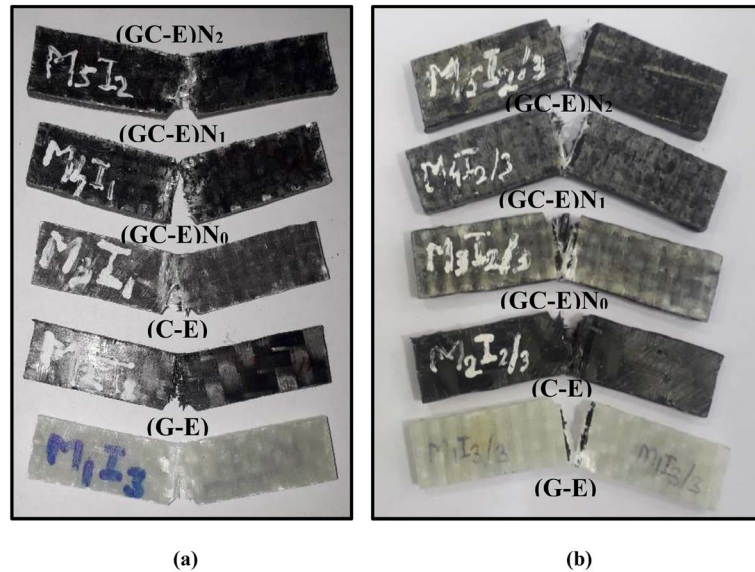


Figure 7. Impact test specimens in (a) dry condition and (b) seawater aged composites.

Figure 7(a) and **Figure 7(b)** depict impact test specimens in dry and seawater-aged conditions. Primary failure occurs on the impacted side of the composites. The plain (G-E) composites exhibit the highest deformation, while plain (C-E) composites show the lowest, linked to the superior strain energy absorption of glass fibers. Consequently, composites with more glass fiber layers demonstrate better impact strength than those with carbon fibers. In seawater-aged conditions, (GC-E)N₁ and (GC-E)N₂ hybrid composites exhibit higher deformation than (GC-E)N₀, enhancing their resilience in both dry and seawater environments.

4. Conclusions

In summary, this study demonstrates the significant enhancements in impact properties and moisture absorption reduction achieved through the synergistic use of hybrid nanofillers (MWCNT + HNT) in epoxy-based glass/carbon composites under dry and seawater-aged conditions. The following inferences are drawn.

- The impact strength degradation of seawater-aged (GC-E)N₀, (GC-E)N₁, and (GC-E)N₂ composites decreased by 12.68%, 11.83%, and 8.52%, respectively, compared to dry-aged specimens.
- The moisture absorption study indicated that the nanofillers modified (GC-E)N₁ and (GC-E)N₂ composites showed notable reductions in moisture absorption content, with decreases of 6.07% and 15.74% respectively, compared to the (GC-E)N₀ composite type. The (GC-E)N₂ type exhibited the least moisture absorption with the lowest diffusion coefficient at 1.287×10^{-3} mm²/hour, showcasing the synergistic impact of MWCNT and HNT hybrid nanofillers. This provides insights into the toughening mechanism and enhanced bonding between the fibers and matrix.

- The application of Fick's Law to model experimental data showcased satisfactory alignment in both linear and saturation regions of moisture absorption for the specimens. Despite minor disparities in outcomes in the intermediate region, the study emphasized a robust correlation with Fick's law, providing insights into the initial phases of moisture absorption mechanisms.

The (GC-E)N₂ composite, reinforced with 2 wt.% hybrid nanofillers, stands out as the optimal choice for marine structural components due to its substantial reduction in moisture absorption and the lowest diffusion coefficients in seawater. This results in superior impact properties and enhanced resilience against environmental factors, such as exposure to seawater, compared to the (GC-E)N₀ composite type. These findings highlight the potential of advanced fiber hybrid composites for use in marine and high-moisture environmental applications, opening up new opportunities for their utilization.

Acknowledgements

Authors would like to thank Sanjay Ghodawat University, Atigre, Kolhapur for providing the required research facilities and support.

Funding

This research received no external funding.

Conflicts of Interest

The authors declare that there is no conflict of interest.

References

- [1] Selvaraju, S. and Ilaiyavel, S. (2011) Applications of Composites in Marine Industry. *Journal of Engineering Research*, No. 2, 89-91.
- [2] Rubino, F., Nisticò, A., Tucci, F. and Carlone, P. (2020) Marine Application of Fiber Reinforced Composites: A Review. *Journal of Marine Science and Engineering*, **8**, Article 26. <https://doi.org/10.3390/jmse8010026>
- [3] Rajak, D., Pagar, D., Menezes, P. and Linul, E. (2019) Fiber-Reinforced Polymer Composites: Manufacturing, Properties, and Applications. *Polymers*, **11**, Article 1667. <https://doi.org/10.3390/polym11101667>
- [4] Rodríguez-González, J.A. and Rubio-González, C. (2021) Seawater Effects on Interlaminar Fracture Toughness of Glass Fiber/Epoxy Laminates Modified with Multi-wall Carbon Nanotubes. *Journal of Composite Materials*, **55**, 387-400. <https://doi.org/10.1177/0021998320950788>
- [5] Mansouri, L., Djebbar, A., Khatir, S. and Abdel Wahab, M. (2019) Effect of Hydrothermal Aging in Distilled and Saline Water on the Mechanical Behaviour of Mixed Short Fibre/Woven Composites. *Composite Structures*, **207**, 816-825. <https://doi.org/10.1016/j.compstruct.2018.09.067>
- [6] Ulus, H., Kaybal, H.B., Eskizeybek, V. and Avci, A. (2020) Halloysite Nanotube Reinforcement Endows Ameliorated Fracture Resistance of Seawater Aged Basalt/Epoxy Composites. *Journal of Composite Materials*, **54**, 2761-2779. <https://doi.org/10.1177/0021998320902821>

- [7] Jesthi, D.K. and Nayak, R.K. (2019) Improvement of Mechanical Properties of Hybrid Composites through Interply Rearrangement of Glass and Carbon Woven Fabrics for Marine Application. *Composites Part B: Engineering*, **168**, 467-475. <https://doi.org/10.1016/j.compositesb.2019.03.042>
- [8] Coleman, J.N., Khan, U., Blau, W.J. and Gun'Ko, Y.K. (2006) Small But Strong: A Review of the Mechanical Properties of Carbon Nanotube-Polymer Composites. *Carbon*, **44**, 1624-1652. <https://doi.org/10.1016/j.carbon.2006.02.038>
- [9] Nurazzi, N.M., *et al.* (2021) Mechanical Performance and Applications of CNTs Reinforced Polymer Composites—A Review. *Nanomaterials*, **11**, Article 2186. <https://doi.org/10.3390/nano11092186>
- [10] Viet, N.V., Wang, Q. and Kuo, W.S. (2016) Effective Young's Modulus of Carbon Nanotube/Epoxy Composites. *Composites Part B: Engineering*, **94**, 160-166. <https://doi.org/10.1016/j.compositesb.2016.03.060>
- [11] Sasidharan, S. and Anand, A. (2020) Epoxy-Based Hybrid Structural Composites with Nanofillers: A Review. *Industrial & Engineering Chemistry Research*, **59**, 12617-12631. <https://doi.org/10.1021/acs.iecr.0c01711>
- [12] Bal, S. and Saha, S. (2017) Effect of Sea and Distilled Water Conditioning on the Overall Mechanical Properties of Carbon Nanotube/Epoxy Composites. *International Journal of Damage Mechanics*, **26**, 758-770. <https://doi.org/10.1177/1056789515615184>
- [13] Nayak, R.K. and Ray, B.C. (2018) Retention of Mechanical and Thermal Properties of Hydrothermal Aged Glass Fiber-Reinforced Polymer Nanocomposites. *Polymer-Plastics Technology and Engineering*, **57**, 1676-1686. <https://doi.org/10.1080/03602559.2017.1419486>
- [14] Crank, J. (1967) *The Mathematics of Diffusion*. Clarendon Press, Oxford.
- [15] Springer, G.S. (1981) *Environmental Effects on Composite Materials*, Vol. 1. Technomic Publishing Company, Lancaster.
- [16] Fick, A. (1855) Ueber Diffusion. *Annalen Der Physik*, **170**, 59-86. <https://doi.org/10.1002/andp.18551700105>
- [17] Shen, C.H. and Springer, G.S. (1976) Moisture Absorption and Desorption of Composite Materials. *Journal of Composite Materials*, **10**, 2-20. <https://doi.org/10.1177/002199837601000101>
- [18] Rao, R.M.V.G.K., Chanda, M. and Balasubramanian, N. (1984) Factors Affecting Moisture Absorption in Polymer Composites Part II: Influence of External Factors. *Journal of Reinforced Plastics and Composites*, **3**, 246-253. <https://doi.org/10.1177/073168448400300305>
- [19] Jesthi, D.K. and Nayak, R.K. (2019) Evaluation of Mechanical Properties and Morphology of Seawater Aged Carbon and Glass Fiber Reinforced Polymer Hybrid Composites. *Composites Part B: Engineering*, **174**, Article ID: 106980. <https://doi.org/10.1016/j.compositesb.2019.106980>
- [20] Rubio-González, C., José-Trujillo, E., Rodríguez-González, J.A., Mornas, A. and Talha, A. (2020) Low-Velocity Impact Behavior of Glass Fiber-MWCNT/Polymer Laminates Exposed to Seawater and Distilled Water Aging. *Polymer Composites*, **41**, 2181-2197. <https://doi.org/10.1002/pc.25530>
- [21] Alamri, H. and Low, I.M. (2012) Effect of Water Absorption on the Mechanical Properties of Nano-Filler Reinforced Epoxy Nanocomposites. *Materials & Design*, **42**, 214-222. <https://doi.org/10.1016/j.matdes.2012.05.060>